Shared Perception for Connected and Automated Vehicles

Yeojun Kim*,1,2, Luca Onesto*,3, Samuel Tay[1], Lujie Yang[1], Jacopo Guanetti[2], Sergio Savaresi[3],
Francesco Borrelli[1]

Abstract— **Connected and automated vehicles (CAVs) have the potential to improve the safety of automated driving by utilizing increased awareness about their surroundings in real time vehicle control. In this paper we propose a framework for a shared perception system suitable for CAVs and explain the algorithms used in the system. Finally, we experimentally demonstrate the benefit of our shared perception system for automated vehicles in uncertain environments.**

I. Introduction

Perception systems are essential in the development and operation of an autonomous vehicle (AV) and Advanced Driver Assistance System (ADAS). AV/ADAS perception systems generally utilize a set of on-board sensors such as camera, radar, and lidar. In recent years, there have been growing efforts from both the research community and the industrial sector to advance on-board sensor technologies and perception algorithms [1]. However, perception systems that rely solely on on-board sensors are inherently limited by the detection range and field of view of their components. These limitations increase uncertainty in the motion planning and control algorithms, which in turn sacrifice performance (passenger comfort, road throughput, energy efficiency) in order to guarantee safety. Communication and connectivity in CAVs can mitigate these shortcomings by enabling real-time control and planning with increased awareness, routing with micro-scale traffic information, coordinated platooning using traffic signals information, and eco-mobility on demand with guaranteed parking enabling rapid cooperative movements [2].

Connected Vehicle (CV) technology is well-established in the automotive community. Dedicated Short Range Communication (DSRC) established highly secure, high-speed direct communication between vehicles and nearby infrastructure [3]. This enables a Vehicular Ad-hoc Network (VANET) which provides Vehicle-to-vehicle (V2V) communication through on-board units (OBU) and vehicle-to-infrastructure (V2I) communication through road-side units (RSU) [4]. DSRC was developed with a primary focus on safety applications, and is based on relatively small packets that are transmitted with low latency; bandwidth limitations would emerge when trying to exchange larger amounts of data. Recently, the fifth generation mobile technology standard (5G) has been proposed as an alternative technology for V2V communication, which would also allow to exchange larger quantities of data [5].

V2V communication can improve vehicle safety by enabling all CVs to share their location and the targets detected by their perception systems. We refer to this concept, which to our best knowledge was first investigated in [6], [7], as *shared perception*. A shared perception system presents each CV with an augmented version of its on board perception system, in which the size of the occluded regions is reduced and the detection range and field of view are increased. Different approaches to shared perception through V2V communication have been explored in the literature. In [8], CVs share and merge their occupancy grid maps using a so-called coordination transformation method. However, the performance of this map merging method is limited at scale, as the large amount of shared data increases the communication delay uncertainty. In [9], the authors propose an object-based approach to shared perception, where the raw data of each detected obstacle is first processed and filtered locally, and subsequently transmitted to the nearby vehicles. The processed obstacle data is abstracted as an *object* with states such as location, velocity, and heading angle measurements and the corresponding covariance matrices, reference frame, etc. This object-based shared perception approach provides main two benefits. First, it can reduce the communication burden by avoiding transmitting raw sensor data. Second, it improves system modularity, i.e. existing on-board sensors can be replaced or new hardware can be added without restrictions on specific hardware, as long as its raw perception data can be represented in a way that fully defines an *object* class defined above. For these reasons, the shared perception system proposed in this paper also implements an object-based shared perception concept.

Other implementations of object-based shared perception are also explored in literature. In [9]–[11], inter-vehicle object association is presented by applying point matching algorithms after taking care of temporal and spatial alignments of CVs and their perceived and shared objects. In [12], driver warnings were demonstrated to alert drivers of potentially dangerous situations using objects perceived by CVs. To the best of the authors' knowledge, the existing literature does not include any demonstration of vehicle motion control based on shared perception with exception of the work in [13] where wireless communications are used only for high level coordination and an on-board lidar and GPS are used

* These authors equally contributed to this work.

[1] These authors are with the Department of Mechanical Engineering, University of California at Berkeley, Berkeley, CA 94701, USA { yk4938, samueltay, yanglujie, fborrelli }@berkeley.edu

[2] These authors are with AV Connect Inc, Alameda, CA 94502, USA { kimyeojun, jacopoguanetti }@gmail.com

[3] These authors are with the Dipartimento di Elettronica Informazione e Bioingegneria, Politecnico di Milano, via G. Ponzio 34/5, 20133 Milan, Italy { luca.onesto,sergio.savaresi }@polimi.it

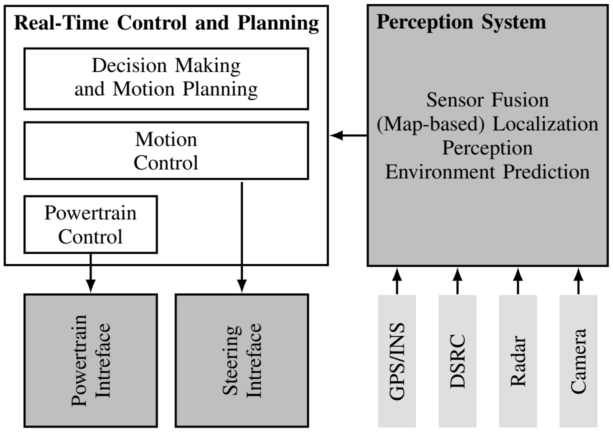

Fig. 1: The on-board perception and control architecture for CAV

for perception and localization.

The contributions of this work are two-fold. First, we propose an object-based shared perception system in order to reduce occluded regions on the road and improve safety. This is accomplished by expanding the standard DSRC message set ([14]) with custom V2V messages, and by a set of algorithms for object fusion and vehicle localization algorithms which are described later in this paper. Second, we experimentally demonstrate a longitudinal motion controller for CAVs that leverages the shared perception system to safely adjust the vehicle speed even before the undetected vehicle suddenly appears in direct line-of-sight.

II. Shared Perception Structure and Algorithms

In this section we introduce the proposed object-based shared perception system. We utilize on-board camera and radar sensors and communicate object-level information about their detected targets through V2V OBUs. Clearly any set of available sensors can be used in our approach.

A. CAV System Structure

Our CAV uses an on-board perception and control architecture suggested by [2] and is shown in Fig. 1. The CAV perception system (upper-right block) receives real-time data from GPS, DSRC, radar, and camera devices and reconstructs the driving situation (e.g. position and speed of surrounding/communicating vehicles, road geometry, traffic lights, etc). This information is then used by the Real-Time Control and Planning system (upper-left block) to compute a safe vehicle trajectory, and the corresponding control inputs are requested to the vehicle actuators through the powertrain and steering interfaces. Readers are encouraged to read [2] for a comprehensive survey of control and planning algorithms that fit in this architecture, particularly for the improvement of energy efficiency and safety.

B. Shared Perception System Structure and Algorithms

Fig. 2 illustrates the shared perception structure of the host vehicle, which refers to the vehicle being controlled and communicating with the other vehicles, next denoted as “peer vehicles”. As illustrated in the figure, perception data from on-board sensors and V2V data from DSRC undergo a set of filtering and object-association steps to construct a set of tables, namely *target table*, *merge table*, and finally *persistent table*. Targets in “Persistent Table” are interpreted as obstacles in motion control of our CAV. A similar approach is proposed in [11].

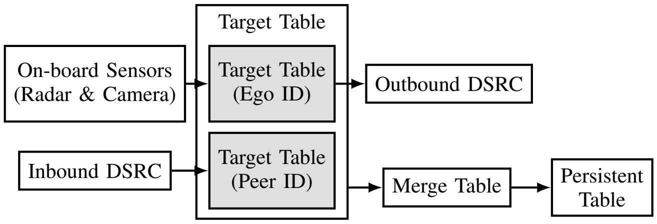

Fig. 2: The shared perception system structure of the host vehicle

Next we explain the steps and algorithms that constitute our proposed shared perception system. For simplicity, we focus on the simplest case with only two communicating vehicles (the host and the peer), although the approach generalizes to cases with more communicating vehicles.

First, assume a set of targets is locally perceived by the on-board radar and camera in the host vehicle. Each target, denoted as z, carries information about its validity (a flag to indicate whether the target is persistently detected and has reasonable measurements), relative position, and relative velocity; Note that this set of information is directly available via communication with the on-board radar and camera modules. We denote the list of radar targets as $\mathbf{z_r}$ and the list of camera targets as $\mathbf{z_c}$. Algorithm 1 details the steps to construct the Target Table for the host vehicle, denoted as $\mathcal{T}^{\text{host}}_{\text{target}}$, using $\mathbf{z_r}$, $\mathbf{z_c}$, GPS information of the two vehicles, and the V2V message such as the target table from the peer ($\mathcal{T}^{\text{peerID}}_{\text{target}}$). At each iteration with time intervals of duration t_s, each target from $\mathbf{z_r}$ and $\mathbf{z_c}$, if it is valid, is associated with the host ID and sorted in an ascending order of relative longitudinal distance (Δy) from the host vehicle. Finally, targets with host ID in $\mathcal{T}^{\text{host}}_{\text{target}}$ are transmitted to other communicating vehicles along with the GPS information of the host vehicle.

Upon receiving its target table information from the peer vehicle, denoted as $\mathcal{T}^{\text{peerID}}_{\text{target}}$, each target in $\mathcal{T}^{\text{peerID}}_{\text{target}}$ is transformed into the host vehicle's reference frame using the host vehicle's GPS and the peer vehicle's GPS (see [9] for example). This step is denoted as changeCoordinate() in Algorithm 1 and can be improved by additionally using local radar data. Section. III explains this step in detail. Finally, the transformed targets are appended to $\mathcal{T}^{\text{peerID}}_{\text{target}}$.

The next step is to construct the Merge table and the Persistent table, denoted as $\mathcal{T}_{\text{merge}}$ and $\mathcal{T}_{\text{persist}}$, respectively. Algorithm 2 details the steps to construct them using $\mathcal{T}^{\text{host}}_{\text{target}}$. At each time stamp, we obtain $\mathcal{T}_{\text{merge}}$ by scanning all the targets and removing all (objects that are identified as) duplicates in $\mathcal{T}^{\text{host}}_{\text{target}}$. This step of finding and removing duplicate

Algorithm 1 Target Table Update for Host Vehicle

```
Input $lat_{\text{host}}$, $lon_{\text{host}}$, $V_{\text{host}}$, $\theta_{\text{host}}$, $lat_{\text{peer}}$, $lon_{\text{peer}}$, $V_{\text{peer}}$, $\theta_{\text{peer}}$, $\mathbf{z_R}$, $\mathbf{z_C}$, $\mathcal{T}^{\text{peerID}}_{\text{target}}$
Output $\mathcal{T}^{\text{host}}_{\text{target}}$
for each iteration, do
    for every target $z$ in $\mathbf{z_R}$ and $\mathbf{z_C}$, do
        if $z$ is valid,
            $z$.host = hostID
            append $z$ to $\mathcal{T}^{\text{host}}_{\text{target}}$
    sort($\mathcal{T}^{\text{host}}_{\text{target}}$) according to $\Delta y$
    $\mathcal{T}^{\text{hostID}}_{\text{target}}$ = [ $q$ in $\mathcal{T}^{\text{host}}_{\text{target}}$ if $q$.host = hostID]
    Transmit $\mathcal{T}^{\text{hostID}}_{\text{target}}$ with $lat_{\text{host}}$, $lon_{\text{host}}$, $V_{\text{host}}$, $\theta_{\text{host}}$

    for every target $q$ in $\mathcal{T}^{\text{peerID}}_{\text{target}}$, do
        changeCoordinates($q, lat_{\text{host}}, lon_{\text{host}}, V_{\text{host}}, \theta_{\text{host}},$
                          $lat_{\text{peer}}, lon_{\text{peer}}, V_{\text{peer}}, \theta_{\text{peer}}$)
        append $q$ to $\mathcal{T}^{\text{host}}_{\text{target}}$
```

targets is denoted as isNeighbor() in the algorithm. In this work we simply use a distance-based method to find the target duplicates (i.e. whether the two targets are within a close proximity, d_c) and remove them. Existing literature is full of alternative and more sophisticated object association methods [10], [11], [15], [16] which can be applied to our framework as well. Finally, we update $\mathcal{T}_{\text{persist}}$ by propagating the target states using a Kalman filter with a 2-D space point-mass model assuming constant velocity and using new measurements in the updated $\mathcal{T}_{\text{merge}}$. In this step, we remove targets that are older than (i.e, no new measurements for more than) n_a time steps. Note that the parameters in our proposed algorithms such as n_a, kalman gains, and d_c are tuning parameters which can differ from each vehicle due to its different sensor specifications.

III. Peer/Target Localization

In the proposed shared perception system, each target seen by a peer vehicle is transformed into the host vehicle's Reference Frame (RF) using the GPS information from the two vehicles via the function changeCoordinate(). As a result, accurate localization of the communicating peer vehicles is critical for the quality of the proposed shared perception system. The proposed method is based on an Extended Kalman Filter (EKF) approach that merges the information provided by a kinematic vehicle model and the radar and GPS measurements of each vehicle. The output of the EKF is the estimated distance between the vehicles' chassis. For the sake of simplicity, two identical cars are considered in this work.

Figure 3 shows the schematic of the proposed approach. The EKF provides the relative distance between the vehicles' chassis and their orientations. The radar and GPS measurements are processed respectively by the *Radar Data Module* and the *GPS Data Module*. Note that these blocks also depend on the current estimate.

Algorithm 2 Merge Table and Persistent Table Updates

```
Input $\mathcal{T}^{\text{host}}_{\text{target}}$
Output $\mathcal{T}_{\text{merge}}$, $\mathcal{T}_{\text{persist}}$
initialize $\mathcal{T}_{\text{persist}} = []$
for each iteration, do
    initialize $\mathcal{T}_{\text{merge}}$ =[]
    for every target $z$ in $\mathcal{T}^{\text{host}}_{\text{target}}$, do
        if isNeighbor($z$, Ego), remove $z$ from $\mathcal{T}^{\text{host}}_{\text{target}}$
        else if isNeighbor($z$, Peer), remove $z$ from $\mathcal{T}^{\text{host}}_{\text{target}}$
        else append $z$ to $\mathcal{T}_{\text{merge}}$
        for every target $q$ in $\mathcal{T}^{\text{host}}_{\text{target}}$, do
            if isNeighbor($z$, $q$), remove $q$ from $\mathcal{T}^{\text{host}}_{\text{target}}$
    for $p$ in $\mathcal{T}_{\text{persist}}$, do
        for $m$ in $\mathcal{T}_{\text{merge}}$, do
            if isNeighbor($m$, $p$),
                kalmanUpdate($p$,$m$)
                $p.age = 0$
                remove $m$ from $\mathcal{T}_{\text{merge}}$
                break
        if $p.age > n_a$, remove $p$ from $\mathcal{T}_{\text{persist}}$
        constantVelocityUpdate($p$)
        $p.age++$
    for $m$ in $\mathcal{T}_{\text{merge}}$, do
        $m.age = 0$
        append $m$ to $\mathcal{T}_{\text{persist}}$
```

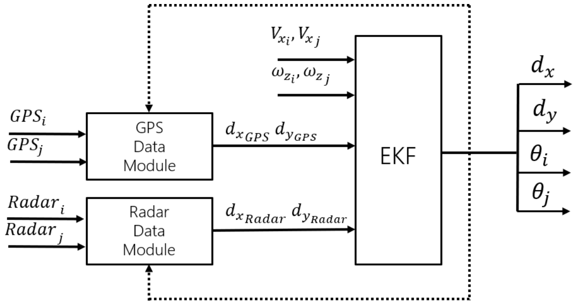

Fig. 3: Schematic of the proposed localization algorithm. Vehicle i and j indicate the host and peer vehicles, respectively.

A. Experimental Setup for Sensors and Communication

The test vehicles are approximated to be a rectangle of length l and width w. They are equipped with a front facing Mando camera and Delphi ESR radar for perception, and a Cohda MK5 OBU, which includes a DSRC radio for V2V communication and a GPS unit (placed in the center of the rectangle) for localization. The vehicles are also equipped with an OTS RT2002 system, a high precision 6 degree of freedom Inertial Measurement Unit (IMU), of which, in the following analysis, only the yaw rate measurement ω_z is considered. The MK5 Unit exchanges DSRC messages according to the SAE J2735 Message Set Dictionary [3], with some customization in order to communicate target information in the Target table.

B. Vehicle Model

In the *Global RF*, the motion of vehicle i is described by the kinematic bicycle model:

$$\begin{cases} x_i(k+1) = x_i(k) + t_s(V_{x_i}(k)\cos(\theta_i(k))) \\ y_i(k+1) = y_i(k) + t_s(V_{x_i}(k)\sin(\theta_i(k))) \\ \theta_i(k+1) = \theta_i(k) + t_s(\omega_{z_i}(k)) \end{cases} \tag{1}$$

where t_s is the sampling time; the inputs of the system are the longitudinal speed V_x in $[m/s]$ and the yaw rate ω_z in $[deg/s]$; the state of the system consists of the pose of the vehicle, where x and y are in $[m]$, and θ which is the heading expressed in $[deg]$. The *Global RF* is aligned with the *GPS RF*, hence the heading θ of the model is consistent with the one measured by the GPS. The model describes the position of the center of the vehicle. Note that the presented kinematic model is suitable for vehicles in lower speed urban or highway environments. In case of highly dynamic sport driving, a more detailed vehicle model should be considered. The distance d between vehicle i and vehicle j involves two components in the *Global RF*, $d_x = x_i - x_j$ and $d_y = y_i - y_j$. Through the kinematic model (1) it is possible to describe their evolution:

$$\begin{cases} d_x(k+1) = d_x(k) \\ \qquad\qquad +t_s(V_i(k)\cos(\theta_i(k)) - V_j(k)\cos(\theta_j(k))) \\ d_y(k+1) = d_y(k) \\ \qquad\qquad +t_s(V_i(k)\sin(\theta_i(k)) - V_j(k)\sin(\theta_j(k))) \\ \theta_i(k+1) = \theta_i(k) + t_s(\omega_{z_i}(k)) \\ \theta_j(k+1) = \theta_j(k) + t_s(\omega_{z_j}(k)) \end{cases} \tag{2}$$

where d_x, d_y, θ_i and θ_j are the state variables of the system, V_i, V_j, ω_i and ω_j are the inputs of the system.

1) Radar measurement: The vehicle's radar provides the distance between the sensor and the detected object in polar coordinates, where ρ is the relative distance and θ_R is the angle. Figure 5a shows the relationship between the (valid) radar measurement and the distance projections d_x and d_y. When the radar of i detects j, the relationship between the state variables and radar measurement is: $d_x = \rho\cos(\theta_i + \theta_R)$, $d_y = \rho\sin(\theta_i + \theta_R)$.

2) GPS measurement: The GPS provides the latitude Lat and longitude Lon of the vehicles. The distance between the GPS coordinates of the two vehicles is calculated as

$$d_{GPS} = R_E \cdot \sqrt{\Delta_{Lon}^2 + \Delta_{Lat}^2} \tag{3}$$

where

$$\Delta_{Lon} = R_E(Lon_i - Lon_j) \cdot \cos\left(\frac{Lat_i + Lat_j}{2}\right)$$
$$\Delta_{Lat} = R_E(Lat_i - Lat_j)$$

and R_E is the earth's mean radius (i.e. $6371 \cdot 10^3$ $[m]$).

Since the GPS modules are installed in the center of the cars, the distance calculated according to (3) also includes part of the chassis of both vehicles. To calculate the distance between the two chassis, a distance correction term is required. The proposed method is a function of the vehicle dimensions, l and w, the distances d_x and d_y and the heading angles θ_i and θ_j.

The two cars can be represented in the vehicle i RF (see Figure 5b). Since the vehicle length l and width w are constant, and they are known a priori, the correction term is a function f of angles γ_1 and γ_2. The overall correction term Δ_{GPS} can be obtained as:

$$\Delta_{GPS} = f(\gamma_1) + f(\gamma_2)$$

where

$$\gamma_1 = \arctan\left(\frac{d_y}{d_x}\right), \gamma_2 = \gamma_1 + 180 - (\theta_i - \theta_j)$$

Figure 4 shows function f for $l = 4.47\,[m]$ and $w = 1.82\,[m]$. Finally, the distance components are obtained as

$$d_x = (d_{GPS} - \Delta_{GPS})\cos(\theta_i - \theta_j)$$
$$d_y = (d_{GPS} - \Delta_{GPS})\sin(\theta_i - \theta_j)$$

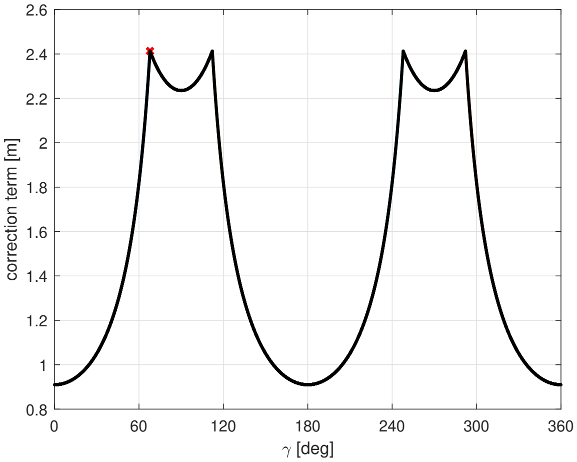

Fig. 4: GPS distance correction term: the correction term in function of γ_1. The red cross represent the maximum value.

3) Experimental Results: The sensor fusion is performed through an EKF framework, where the information provided by the sensors are compared with the nonlinear kinematic model (2).

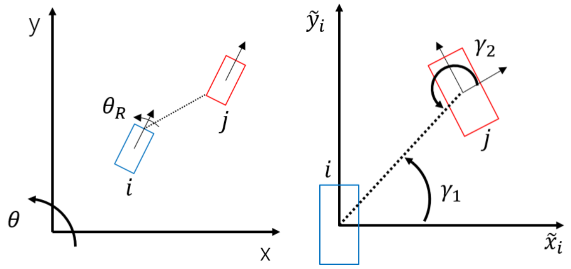

(a) Global RF

(b) Vehicle i RF

Fig. 5: Cars displacement with the radar measurements (a) in the *Global RF* and (b) in the vehicle i RF.

Figure 6 shows an experimental test performed with two identical cars. The test protocol is the following:

- The two cars are sitting still, side by side;
- Vehicle i reaches the constant speed of 7 $[m/s]$ on a straight path;
- Vehicle j follows vehicle i and then performs an overtaking maneuver;
- Vehicle j reaches the constant speed of 7 $[m/s]$.

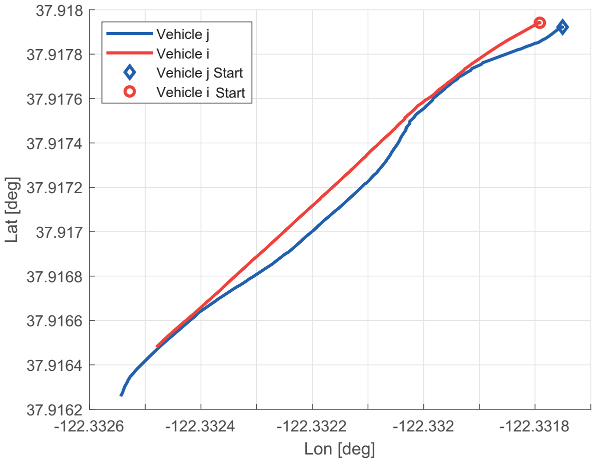

Fig. 6: Experimental results: path logged by the GPS during an overtaking maneuver

Figure 7 shows in the top plot the vehicles speed, while the bottom plot shows the estimated distance by the proposed approach and the raw distance measured by the GPS.

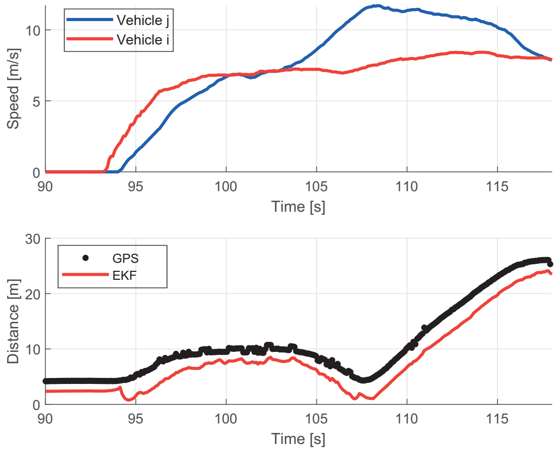

Fig. 7: Experimental results: measured speed and estimated distance

Note the following remarks from the results:

- The estimated distance has the same profile as the measured one.
- The difference between the two signals is due to the correction term. In fact, the proposed approach takes into consideration the dimensions of the chassis. This improvement can be useful to increase the safety and prevent accidents.

IV. Experimental Demonstration with Longitudinal Motion Controller

In this section we demonstrate the proposed perception system with a closed loop longitudinal motion controller. We will consider an intersection with large areas of occlusion to demonstrate the advantage of our shared perception system when the presence of obstacles is uncertain, as illustrated in fig. 8. The host vehicle, of which the longitudinal motion is controlled, communicates with the peer vehicle. The non-communicating vehicle (red) is entering the intersection and cutting in while occluded to the ego vehicle but seen by the peer vehicle.

Sensor and communication setups for the host and the peer vehicles are the same as explained in Sec. III-A. Moreover, to execute the shared perception algorithms and the longitudinal motion control in real-time, the host vehicle is also equipped with a Matrix embedded PC-Adlink (MXC-6101D/M4G with Intel Core i7-620LE 2.0 GHz processor) with Robot Operating System (ROS) and dSpace MicroAutoBox (IBM PowerPC 750FX processor, 800 MHz).

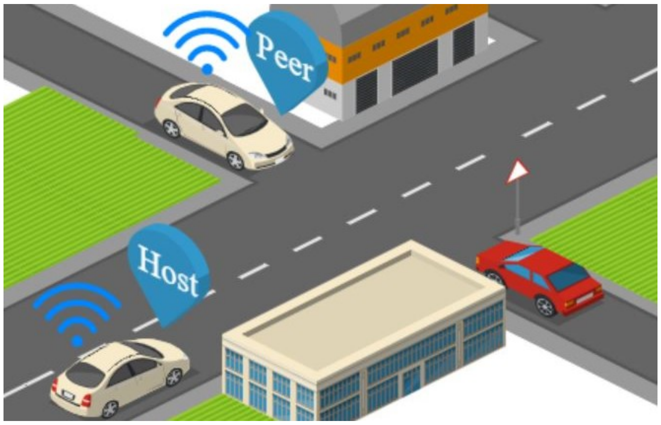

Fig. 8: Illustration of the Experimental Setup

A. Longitudinal Motion Controller Design

As shown in Fig. 1, our CAV executes the longitudinal motion control by exploiting real-time perception information from the DSRC, as well as the on-board sensors such as radar and camera. Our longitudinal motion controller, which commands the reference wheel torque, is based on the model predictive control based adaptive cruise control design proposed in [17]. The only difference is that the distance to the front vehicle is obtained by taking the minimum distance of the targets that are in the Persistent table and entering the host vehicle's path. To determine whether a target will enter the host vehicle's path, we check if the following conditions are met.

$$[x_{\text{host}}, x_{\text{host}} + HV_{x,\text{host}}] \cap [x_{\text{target}}, x_{\text{target}} + HV_{x,\text{target}}], \tag{4a}$$

$$[y_{\text{host}}, y_{\text{host}} + HV_{y,\text{host}}] \cap [y_{\text{target}}, y_{\text{target}} + HV_{y,\text{target}}] \tag{4b}$$

where H is the planning horizon time.

B. Results and Discussion

Fig. 9 shows the trajectories of the ego vehicle in terms of the relative distance to the vehicle on the host vehicle's path, velocity, and reference torque input. Note that our experiment was conducted at a low speed (less than $5\,[m/s]$). In this scenario, our share perception system can feed the relative distance to the front vehicle about 3.5 seconds earlier than when the sensor fusion of the on-board sensors (camera and radar). This allows the longitudinal motion controller to react to the possible vehicle cut-in early enough to maintain a safe distance. It is also noted that our shared perception momentarily loses a target at time instant 5 causing aggressive torque input. Designing more robust objection association (isNeighbor()) rather than a simple distance-based method in our shared perception algorithms to avoid this kind of situation remains to be our future work.

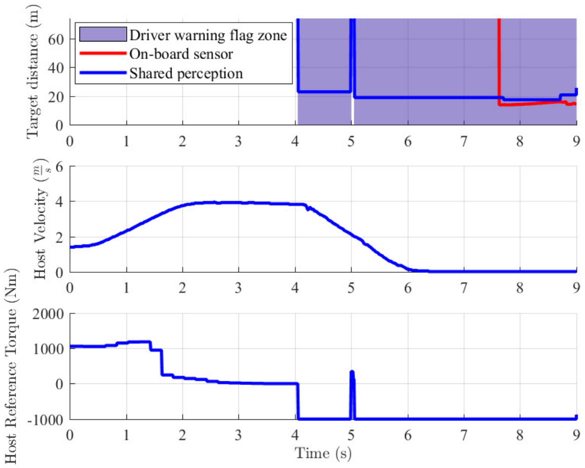

Fig. 9: Plots of relative distance, velocity, and reference torque.

Video demonstration for various applications of the proposed shared perception system as well as our experiment can be found at [18].

V. Conclusion

In this paper, we propose a framework to achieve a shared perception system for CAVs, and present algorithms for better localization of communicating peers. We show the effectiveness of our shared perception system by demonstrating a longitudinal motion controller which exploits the sensor fusion data from the shared perception system. Our future research will expand this work in two directions. First, more sophisticated methods for target association and measurement updates in our algorithms can be utilized to improve the quality of the shared perception. The experimental validation of the proposed peer vehicle localization in Section. III with dGPS measurements remains as a future work. Second, we plan to apply the shared perception for more complex maneuvers of autonomous vehicles such as lane changing, intersection crossing, platooning, etc.

Acknowledgement

The information, data, or work presented herein was funded in part by the Advanced Research Projects Agency-Energy (ARPA-E), U.S. Department of Energy, under Award Number DE-AR0000791. The views and opinions of authors expressed herein do not necessarily state or reflect those of the United States Government or any agency thereof.

References

[1] J. Van Brummelen, M. O'Brien, D. Gruyer, and H. Najjaran, "Autonomous vehicle perception: The technology of today and tomorrow," *Transportation research part C: emerging technologies*, vol. 89, pp. 384–406, 2018.

[2] J. Guanetti, Y. Kim, and F. Borrelli, "Control of connected and automated vehicles: State of the art and future challenges," *Annual Reviews in Control*, vol. 45C, pp. 18–40, 2018.

[3] J. B. Kenney, "Dedicated short-range communications (dsrc) standards in the united states," *Proceedings of the IEEE*, vol. 99, no. 7, pp. 1162–1182, 2011.

[4] S. Al-Sultan, M. M. Al-Doori, A. H. Al-Bayatti, and H. Zedan, "A comprehensive survey on vehicular ad hoc network," *Journal of network and computer applications*, vol. 37, pp. 380–392, 2014.

[5] X. Cheng, C. Chen, W. Zhang, and Y. Yang, "5g-enabled cooperative intelligent vehicular (5genciv) framework: When benz meets marconi," *IEEE Intelligent Systems*, vol. 32, no. 3, pp. 53–59, 2017.

[6] M. Roeckl, J. Gacnik, J. Schomerus, T. Strang, and M. Kranz, "Sensing the environment for future driver assistance combining autonomous and cooperative appliances," in *Proceedings*, pp. 45–56, 2008.

[7] F. Ahlers and C. Stimming, "Cooperative laserscanner pre-data-fusion," in *2008 IEEE Intelligent Vehicles Symposium*, pp. 1187–1190, IEEE, 2008.

[8] S.-W. Kim, Z. J. Chong, B. Qin, X. Shen, Z. Cheng, W. Liu, and M. H. Ang, "Cooperative perception for autonomous vehicle control on the road: Motivation and experimental results," in *2013 IEEE/RSJ International Conference on Intelligent Robots and Systems*, pp. 5059–5066, IEEE, 2013.

[9] A. Rauch, F. Klanner, R. Rasshofer, and K. Dietmayer, "Car2x-based perception in a high-level fusion architecture for cooperative perception systems," in *2012 IEEE Intelligent Vehicles Symposium*, pp. 270–275, IEEE, 2012.

[10] A. Rauch, S. Maier, F. Klanner, and K. Dietmayer, "Inter-vehicle object association for cooperative perception systems," in *16th International IEEE Conference on Intelligent Transportation Systems (ITSC 2013)*, pp. 893–898, IEEE, 2013.

[11] M. Ambrosin, I. J. Alvarez, C. Buerkle, L. L. Yang, F. Oboril, M. R. Sastry, and K. Sivanesan, "Object-level perception sharing among connected vehicles," in *2019 IEEE Intelligent Transportation Systems Conference (ITSC)*, pp. 1566–1573, IEEE, 2019.

[12] F. Seeliger, G. Weidl, D. Petrich, F. Naujoks, G. Breuel, A. Neukum, and K. Dietmayer, "Advisory warnings based on cooperative perception," in *2014 IEEE Intelligent Vehicles Symposium Proceedings*, pp. 246–252, IEEE, 2014.

[13] P. Xu, G. Dherbomez, E. Héry, A. Abidli, and P. Bonnifait, "System architecture of a driverless electric car in the grand cooperative driving challenge," *IEEE Intelligent Transportation Systems Magazine*, vol. 10, no. 1, pp. 47–59, 2018.

[14] , *Dedicated Short Range Communication (DSRC) Systems Engineering Process Guidance for SAE J2945/X Documents and Common Design Concepts^{TM}*, 12 2017.

[15] D. Franken and A. Hupper, "Improved fast covariance intersection for distributed data fusion," in *2005 7th International Conference on Information Fusion*, vol. 1, pp. 7–pp, IEEE, 2005.

[16] F. de Ponte Müller, E. M. Diaz, and I. Rashdan, "Cooperative positioning and radar sensor fusion for relative localization of vehicles," in *2016 IEEE Intelligent Vehicles Symposium (IV)*, pp. 1060–1065, IEEE, 2016.

[17] S. Lefevre, A. Carvalho, and F. Borrelli, "Autonomous car following: A learning-based approach," in *2015 IEEE Intelligent Vehicles Symposium (IV)*, pp. 920–926, IEEE, 2015.

[18] Y. Kim and S. Tay, "Shared perception for connected and automated vehicles." `www.youtube.com/watch?v=iBY3RQ1SGDU`, 2020.